Continuous and Fine-grained Breathing Volume Monitoring from Afar Using Wireless Signals

Phuc Nguyen*, Xinyu Zhang†, Ann Halbower‡, Tam Vu*
*University of Colorado, Denver, †University of Wisconsin-Madison, ‡University of Colorado School of Medicine
{phuc.v.nguyen, tam.vu}@ucdenver.edu, xyzhang@ece.wisc.edu, ann.halbower@childrenscolorado.org

***Abstract*—In this work, we propose for the first time an autonomous system, called WiSpiro, that continuously monitors a person's *breathing volume* with high resolution during sleep from afar. WiSpiro relies on a phase-motion demodulation algorithm that reconstructs minute chest and abdominal movements by analyzing the subtle phase changes that the movements cause to the continuous wave signal sent by a 2.4 GHz directional radio. These movements are mapped to breathing volume, where the mapping relationship is obtained via a short training process. To cope with body movement, the system tracks the large-scale movements and posture changes of the person, and moves its transmitting antenna accordingly to a proper location in order to maintain its beam to specific areas on the frontal part of the person's body. It also incorporates interpolation mechanisms to account for possible inaccuracy of our posture detection technique and the minor movement of the person's body. We have built WiSpiro prototype, and demonstrated through a user study that it can accurately and continuously monitor user's breathing volume with a median accuracy from 90% to 95.4% (or 0.058*l* to 0.11*l* of error) to even in the presence of body movement. The monitoring granularity and accuracy are sufficiently high to be useful for diagnosis by clinical doctor.**

I. Introduction

Continuous respiratory rate and volume monitoring play an important role in health care. While an abnormality in breathing rate is a good indication of respiratory diseases such as interstitial lung disease (too fast) or drug overdose (too slow), *fine-grained breathing volume information* adds valuable information about the physiology of disease. Common obstructive airway diseases such as asthma and chronic obstructive pulmonary disease (COPD), for example, are characterized by the decreased flow rate measure at different breathing volumes. A constant loss of lung volume in these diseases not only indicates acute changes in the disease stability but also reveals lung remodeling and other irreversible states of diseases. Further, patients with lower airway diseases such as cystic fibrosis or tuberculosis could be diagnosed when sudden drops in breathing volume are frequently detected [1]. Therefore, accurate and fine-grained breathing volume measurements could offer rapid and effective diagnostic clues to the development of disease progression [2].

Being able to unobtrusively and continuously monitor lung volume has a high clinical impact. In many instances, patients with respiratory disease only show their symptoms for a short period and at a random time. In another important health care practice, breathing volume of prematurely-born, or preterm, babies needs to be closely and continuously monitored. A decrease of the babies' breathing flow and volume must be promptly detected well before it causes oxygen desaturation for doctors to give an effective neonatal ventilation intervention. In a recent study on the effects of sleep apnea during pregnancy [3], it has been shown that detection of sleep-disordered breathing is possible in women who did not have sleep apnea prior to pregnancy, and that apnea leads to abnormal pregnancy outcomes [4]. In these cases, many only develop apnea for a short period of time. Hence, monitoring them non-invasively over a longer term to detect lung volume changes is critical. Last, but not least, long-term monitoring of breathing volume during sleep detects sleep-related breathing disorders common in 5% of children and 10-40% of adults population [5], [6]. Fine-grained and continuous breathing volume information will help classifying different types of hypopnea (partial airflow obstruction common in children) during sleep to better define the abnormality and direct proper treatment strategies where obstructive hypopnea is treated differently than central apnea [7]. In all above mentioned health care practices, the detection of disease and the observation of disease progression or remission could only be viable with an accurate and fine-grained breathing volume monitoring technique over an extended period of time.

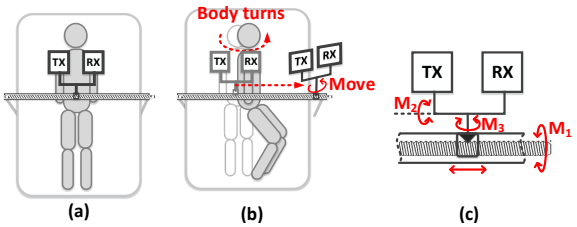

Fig. 1. The conceptual design of WiSpiro. A radar beams to human's heart area to observe the respiratory and heart beat activities, as shown in (a). If a body movement or posture change is detected during sleep, the radar is then moved to a new location and redirects its radio beam to maintain its orientation pointing to the heart area, as shown in (b).The radar navigator could roll, pitch, and yaw with 360 degree of freedom using three motors M_1, M_2, and M_3 to control antennas' position and their beaming directions, as shown in (c).

Current practice for long-term breathing volume monitoring is obtrusive: airflow are measured from the nose and mouth qualitatively or at best semi-quantitatively with pressure manometers or impedance chest belt [7]. Non-obtrusive approaches are apparently more attractive and usable. So far, however, the literature has mainly focused on the problem of *breathing rate* estimation using camera [25], laser [20], [28], infrared (IR) signal [8], earphones [9], and most recently using

978-1-4673-9953-1/16/$31.00 ©2016 IEEE

radio signals [10]–[14]. While these breathing rate estimation solutions are accurate and practical, little progress has been made along the line of breathing volume estimation. Massagram *et al.* [19] presented a technique to calculate breathing volume of a person from radio signal reflected off the subject's chest. While the technique is promising and works with a static subject, it is not applicable for long-term monitoring where subject movement is unavoidable. Moreover, it can only estimate breathing volume once in every breathing cycle.

This paper introduces *WiSpiro*, a system that uses directional radios to continuously monitor a person's breathing volume with high resolution during sleep from afar. WiSpiro relies on a phase-motion demodulation algorithm that reconstructs minute chest and abdominal movements by analyzing the subtle phase changes that the movements caused to the continuous wave signal beamed out by WiSpiro, as shown in Fig. 1(a). These movements are used to estimate breathing volume, whose relationship is obtained via a short neural-network training process. The key property of WiSpiro is the ability to work with the presence of random body movement. WiSpiro autonomously tracks the large-scale movements and posture changes of the person, and moves its transmitting antenna accordingly to a proper location in order to maintain its beam to specific areas on the frontal part of the persons body, as conceptually illustrated in Fig 1(b) and (c). It also incorporates interpolation mechanisms to account for possible inaccuracy of our posture detection technique and the minor movement of the subject's body.

We have built WiSpiro prototype and demonstrated its potential through a user study that it can accurately and continuously monitor user's breathing volume with a median accuracy from 90% to 95.4% even in the presence of body movement. Our results also show granularity of the estimation is sufficiently high to be useful for sleep study analysis. They key findings and contributions of this paper are as follows:

- Theoretical and practical design of a breathing volume estimator. We derive a model for the effects of chest movement and posture change on radar signals in terms of phase and signal strength. We adopt a calibration technique inspired by neural network back propagation training model to calculate breathing volume from the chest movement (Sec. IV).
- A set of algorithm to address challenges caused by body and body part movement. Posture detection and point localization techniques are developed to guide the antenna movement and orientation when movement occurs. To improve the correctness of inferring breathing volume from chest movement, an interpolation technique is introduced to integrate with the point localization output which helps correcting the estimation results (Sec. V).
- Implementation and evaluation show the feasibility, performance, and potential of the system. We propose and implement 4 algorithms including chest movement reconstruction, posture estimation, point localization, and volume interpolation on our prototype. We conducted experiment on 6 users for 360 minutes and report the results. The results show high estimation accuracy after integrating of the 4 above-mentioned optimization techniques (Sec. VII).

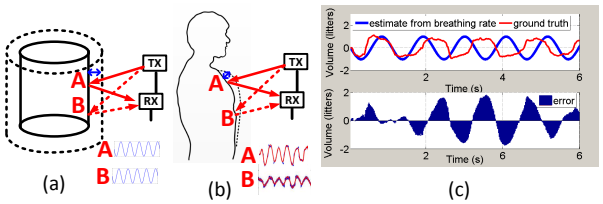

Fig. 2. An illustration of the problem of approximating breathing volume using rate, and inferring breathing volume from untrained areas.

II. WiSpiro Goals and Challenges

WiSpiro is designed to be able to *unobtrusively and autonomously* estimate the *breathing volume* with *fine-granularity at sub-breathing cycle level* even with the presence of random body movements. Next, we will discuss challenges in realizing such goals including the ones caused by the nature of breathing activities and non-uniformed shape of human chest areas, by body movement, and the nature of radio signals.

Nonuniform movement of body areas during breathing. Due to the non-uniform physical shape of human rib cage and upper body, the movement of different areas on human chest caused by respiratory activities are also non-uniform. Fig. 2 illustrates the non-uniformity of a human chest in contrast with a uniform surface of a cylinder. Given the same volume change, all points on the cylinder will move with the same distance. On the other hand, when a normal person inhales or exhales a certain volume, the xiphoid process area moves with a smaller amplitude compared to the movement of the right chest or left chest area, as shown in prior work in human anatomy [23]. This implies that the relationship between chest movement and breathing volume is non-uniform across different chest areas. Because of this property, even a minor non-respiratory movement of the body could make the antennas point to a wrong location which could cause significant volume estimation error. Therefore, at any given time, WiSpiro must be able to distinguish the area that it is beaming to in order to estimate breathing volume with high accuracy. To that end, we choose to adopt highly directional radar transceivers, and develop a posture detection algorithm to detect the cross section vector of human chest movement. Next, we build an autonomous motion control system which is able to direct the antennas towards a fixed anchor area (*e.g.*, heart area) to monitor human chest movement. We present the solutions in Sec. V-A.

Possible blockage of radio signals. During sleep, a subject might change her posture or move her body part to react to common environmental events such as random loud sound, change of temperature, humidity, and light condition, etc. These changes or body part's movements (*e.g.*, arms) might block the anchor area (*e.g.*, heart area) from the light-of-sight of the antennas. Therefore, WiSpiro needs to find an alternative area which can be seen clearly by radar. It then infers the breathing volume based on the movements captured on that area and the relationship between that movement and

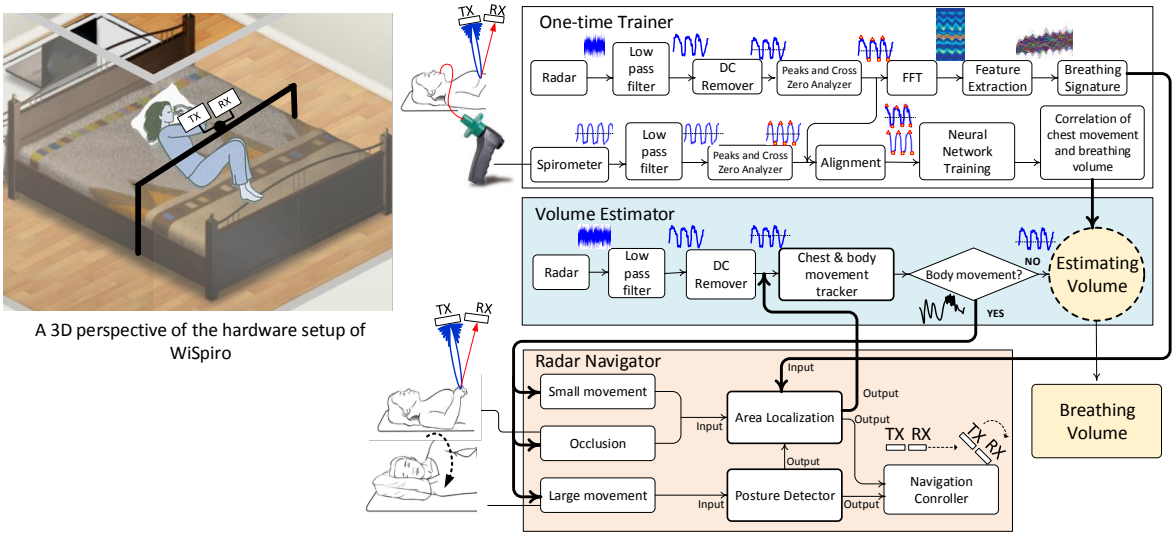

Fig. 3. Architectural overview of WiSpiro.

breathing volume learned in the one-time training process at the beginning. We present the solution to this problem in Sec. V-B.

Non-linear relationship between chest movement and breathing volume. It is seemingly possible to obtain breathing volume from the rate by assuming that the breathing volume has a form of $V = Asin\omega t$, where V is the breathing volume, A is the amplitude that could be obtained by calibration, and $\omega = 2\pi f$ (f is the breathing rate) [11]. However, this model misses the inhaled and exhaled patterns of breathing activities. A brief experiment has been conducted to evaluate the possibility of this approach. The results (Fig. 2 (a)) show that the actual breathing volume does not follow a perfect sinusoidal form in each cycle. However, the imperfect curve is of interest to medical practitioners because it reflects the subject's breathing patterns. The respiration volume information is buried in the very minor phase shift of the reflected signal. This is in sharp contrast with respiration rate which only needs to extrapolate peak frequency of the respiration curve. To solve this problem, we establish a model to map WiSpiro's received signal pattern to chest movement (Sec. IV), and then map the movement to fine-grained breathing volume value according to a neural network model trained for different chest positions (Sec. IV-D).

In short, there are many challenges on designing a radar system for monitoring the breathing activity continuously, automatically, and with fine granularity. To our knowledge, WiSpiro represents the first system that can meet the challenges, and realize robust breathing volume estimation in practical sleeping environment with random body movement.

III. *WiSpiro* Overview

WiSpiro is created to continuously monitor breathing volume of a subject during sleep. Figure 3 sketches its functional architecture, which includes three main components: *volume estimator*, *radar navigator*, and *one-time trainer*. In the following, we briefly describe these key components.

Volume estimator. WiSpiro builds on a decoding technique that extracts subject's frontal movement due to breathing, heart beat, and random body movement from the reflected radio signals. It continuously tracks the minute frontal body movement by analyzing the phase shift and signal strength of the signal captured by the receiving radar. This movement information is then combined with a prior knowledge, learned through a one-time training process, to estimate fine-grained breathing volume.

Radar navigator. WiSpiro relies on this navigator to address challenges caused by subject's random movement, which could come from limbs, shoulder, other body parts, or the whole body, during sleep. Taking phase-shift and signal strength information from the previous component as inputs, the radar navigator detects large- and small-scale body movement. It *estimates the sleeping posture* of the subject and moves the antenna accordingly to redirect the radio beam to the subject's chest upon detecting body movement. Furthermore, it executes an *area localization* algorithm to identify the area on the chest to which the radio beam is pointing. This area information not only allows the navigator to fine-tune its antenna orientation to beam to the subject's heart area but also informs the volume estimator which training data should be used for calculating the volume. Note that the same breathing behavior can cause different areas to move differently. The last operation of the radar navigator is occlusion detection, *i.e.*, detecting if the heart area is in direct light-of-sight with the transmitter and the receiver. In case when occlusion occurs, it redirects the antenna beam to alternative areas (*e.g.*, lower chest, or abdominal areas) to continue the monitoring process.

One-time trainer. Firstly, a training step is required to establish the correlation between human chest movement and breathing volume because this correlation depends on chest size, age, breathing patterns, and so on. Secondly, the system needs to know exactly where it's pointing, so that it uses the correct correlation function for estimating breathing volume from the chest movement. For the first task, the trainer uses

neural network to establish the relationship between body movement and beaming area with the breathing volume. Given an instance of chest movement at a known area on human chest as an input, the output of the function is a corresponding breathing volume. Lastly, the trainer provides the characteristics of the reflected signal when radar beams to different areas on the human chest. These characteristics are mapped into features. By comparing the features of the signal with those of the signals from trained areas, the system can infer the location at which radar is pointing. We describe in detail the 3 above components in the next sections.

IV. Volume Estimator with Chest Movement Reconstruction

A. Theoretical analysis of movement reconstruction

A WiSprio transmitter continuously emits a single tone signal with frequency ω, and uses a directional antenna to beams the signal towards the subject's chest. When hitting the subject's chest, parts the signal will eventually be captured by a directional receiver radio. The single-tone continuous wave $T(t)$ is formulated as:

$$T(t) = cos(\omega t)$$

Let d_0 be the distance between radar and human chest, $m(t)$ be the chest movement function representing the chest position at time t, then $d(t) = d_0 + m(t)$ will be the effective distance between the radar and human chest at any given chest position at time t. The received signal, namely $R(t)$, can be written as:

$$R(t) = cos\left[\omega\left(t - \frac{2d(t)}{c}\right)\right] = cos\left[\omega\left(t - \frac{2d_0 + 2m(t - \frac{dt}{t})}{c}\right)\right]$$

In the above equation, $\frac{d(t)}{c}$ is negligible since $d(t)$ is 10 orders of magnitude smaller than the speed of light c. Therefore, $m(t - \frac{d(t)}{c}) \approx m(t)$ and, $R(t)$ can be rewritten as:

$$\begin{aligned} R(t) &= cos\left[\omega\left(t - \frac{2d_0}{c} - \frac{2m(t)}{c}\right)\right] \\ &= cos\left(\omega t - \frac{4\pi d_0}{\lambda} - \frac{4\pi m(t)}{\lambda}\right) \end{aligned} \tag{1}$$

As shown in the Eq. (1), the received signal $R(t)$ includes a high frequency component (*i.e.*, at transmitted frequency ω) and a low frequency component caused by chest movement $m(t)$. We are interested in extrapolating the low frequency component which is pertinent to volume estimation.

To do that, we note that the radar mixes its received signal $R(t)$ with the originally transmitted one $T(t)$ using a simple mixer. In an ideal mixer, the output signal, called $B(t)$, is the multiplication of $T(t)$ with $R(t)$ which are the two inputs to the mixer. $T(t)$ is fetched into the mixer via its local oscillator (LO) port. Different frequency components of the output signal from the mixer is calculated as:

$$\begin{aligned} B(t) &= cos(\omega t) cos\left(\omega t - \frac{4\pi d_0}{\lambda} - \frac{4\pi m(t)}{\lambda}\right) \\ &= \underbrace{cos\left(\frac{4\pi d_0}{\lambda} + \frac{4\pi m(t)}{\lambda}\right)}_{\text{low freq. comp.}} + \underbrace{cos\left[\left(2\omega t - \frac{4\pi d_0}{\lambda} - \frac{4\pi m(t)}{\lambda}\right)\right]}_{\text{high freq. comp.}} \end{aligned} \tag{2}$$

Now that the two signal are separated after passing through the mixer, the low frequency component could be retrieved by a simple low pass filter. The filtered signal, called $F(t)$, is written as following:

$$F(t) = cos\left(\frac{\overbrace{4\pi d_0}^{\text{large-scale movement}}}{\lambda} + \frac{\overbrace{4\pi m(t)}^{\text{vital sign movement}}}{\lambda}\right) \tag{3}$$

Note that WiSprio estimates breathing volume only when the subject does not move. If a body movement is detected (discussed in Sec. V), the radar navigator will take control to adjust the antennas to beam to a correct position before restarting the breathing volume estimation process. When the body is static, the distance between the antennas and the subject's frontal areas d_0 remains fixed. Therefore, from Eq. (3), phase change between two consecutive samples, $F(k)$ and $F(k-1)$, represents only chest movement due to vital signals including breathing and heart rate.

$$arctan\Big(F(k)\Big) - arctan\Big(F(k-1)\Big) \approx \frac{4\pi(m(k) - m(k-1))}{\lambda}$$

Let Δm be the chest movement between the two consecutive samples, then $\Delta m = m(k) - m(k-1)$. If $F_I(t)$ and $F_Q(t)$ are the I and Q channels of $F(t)$, respectively, then the above equation can be rewritten as:

$$\begin{aligned} &\frac{4\pi\Delta m}{\lambda} \approx arctan\left(\frac{F_Q(k)}{F_I(k)}\right) - arctan\left(\frac{F_Q(k-1)}{F_I(k-1)}\right) \\ &\Leftrightarrow \Delta m \approx \frac{\lambda}{4\pi}\left(arctan\left(\frac{F_Q(k)}{F_I(k)}\right) - arctan\left(\frac{F_Q(k-1)}{F_I(k-1)}\right)\right) \end{aligned} \tag{4}$$

Eq. (4), shows how chest movement is calculated from samples of received signal. Note that the movement estimation is independent of d_0, which is base distance from chest to antenna.

B. Volume Estimation Algorithm

Based on the prior analysis, we design an algorithm to robustly demodulate fine-grained breathing volume from received signals. Several challenges need to be addressed in this process. First, the respiratory chest movement between two consecutive reflected signal samples is very small and is buried in minor phase change. Second, it is difficult to detect phase changes given the various types of noise in the system which are introduced by reflection from background objects, multipath components, and signal leakage due to TX, RX hardware imperfection. Last but not least, the nonuniform movement of different body areas during breathing makes the correlation between area movement vs. breathing volume to be dependent on the area location.

To overcome the above challenges, we exploit the regularity and quasi-periodic nature of chest area movement. In particular, an area is highly likely to move along the same direction, either inward (exhaling) or outward (inhaling), for a number of sampling cycles before the direction is changed. The intuition is that one cannot alter his or her breathing from inhale to exhale in one sampling cycle and then back. Moreover, the movement direction only changes when the subject changes from inhale to exhale, *i.e.*, finishing one half of a breathing cycle. Thus, we identify and group chest area movements

within one half of a breathing cycle for breathing volume estimation for which per-sample breathing volume is inferred. In addition, we found that the noises are either reflected off rather stationary sources or from hardware leakage, and thus have either relatively low frequencies or frequencies following Gaussian distribution. Therefore, these noises can be removed with proper filtering mechanisms such as DC and band-pass filters. Lastly, a one-time neural-network-based training process is designed to mine the relationship between breathing volume and chest movement for each chest area. These area-specific relationships are later used for volume estimation. Alg. 1 summarizes our basic volume estimator which integrates these solution principles, with the following key steps.

Algorithm 1: Basic Volume Estimation Algorithm

Input : $F_I(k)$ and $F_Q(k)$ /* Received samples */ $S, areaID, L, N_c(areaID)$ /* which are number of samples, chest area ID, moving window size, and trained neural network for $areaID$, respectively/

Output: Estimated breathing volume vector $V^*[1:S]$

$F'_I \leftarrow$ DC filtered of F_I; and $F'_Q \leftarrow$ DC filtered of F_Q

$CZ[1:n] \leftarrow$ Find cross zero indexes of $arctan(\frac{F'_Q}{F'_I}[1:S])$,

for $j = 1$ *to* $n-1$ **do**

  $V[CZ(j):CZ(j+1)] \leftarrow$ $N_c(areaID, arctan(\frac{F'_Q}{F'_I})[CZ(j):CZ(j+1)])$

$V^*[1:S] \leftarrow V[CZ(1):CZ(n)]$

Signal preprocessing. Assuming the signal sequence received by the receiver has S samples which are in I and Q channels and acquired as described in Sec. IV-A. The series of $F_I(k)$ and $F_Q(k)$, $k \in [1:S]$ contains DC components caused by hardware leakage and quasi-stationary background which are removed by a moving-average DC filter. The filtered signal sequence, $F'_I(k)$ and $F'_Q(k)$, are $F'_{I,Q}(t) = F_{I,Q}(k) - \frac{1}{L}\sum_{i=0}^{L}|F_{I,Q}(k-i)|$ in which L is the moving window size and $k \in [1:S]$.

Half-cycle segmentation. The filtered samples are then divided into n segments where n is the number of times that the phase of the signal, $arctan(\frac{F'_Q}{F'_I})$, crosses zero. By doing so, samples of the same breathing activity, either inhale or exhale, are grouped into the same segment. It also accommodates group with different size which mean breathing activity with different paces, such as a long inhale or short exhale.

Per-segment volume estimation. This step is to calculate the volume of each half-cycle segment. One important input of this step is the neural network that contains the relationship between a movement of a specific chest area and its corresponding breathing volume values. This network conducts the one-time training process that is presented in the following subsection, Sec. IV-C. Another key input is the ID of the chest location at which the antennas are beaming.

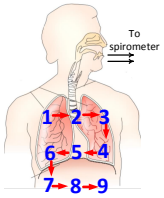

Fig. 4. Movement-to-Volume Training: The subject chest is divided into subareas each.

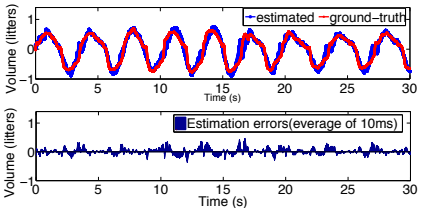

Fig. 5. Breathing volume estimated by the basic WiSpiro algorithm for a stationary person - a mean error of $0.021l$ and maximum error of $0.052l$ and a standard deviation of $0.011l$.

C. Training the Neural Network for Movement-to-Volume Mapping

WiSpiro is built on a physiological premise of the harmonic movement between the chest and lung expansion during breathing. That is, when the lung expanses due to inhaling, the chest is also expanding. Likewise, the chest is collapsing during exhale. This phenomenal is the leading principle for our training algorithm. This training process quantifies the relationship between chest movement and breathing volume of individual. It needs to also take into account the non-uniformity of the movement on different chest areas given the same breathing activity.

Algorithm 2: Training for Movement-to-Volume Neural Network

Input : $F_I(k)$ and $F_Q(k)$ /* Received samples */ $gridSize$ /* Number of chest areas */ N /* Total number of samples collected per area */

Output: Trained neural network $N_c[i]$ for all areas with $i \in [1, gridSize]$

for ***each*** *area* **do**

  $V_G[1:N] \leftarrow$ Volume measured by spirometer for area i

  $f_L \leftarrow 0.2Hz$; $f_H \leftarrow 1.8Hz$; /* Cut-off frequencies */

  $F'_I \leftarrow$ DC filtered of F_I; and $F'_Q \leftarrow$ DC filtered of F_Q

  $F^*[1:N] \leftarrow$ Band pass filter of $(arctan(\frac{F'_Q}{F'_I})[1:N])$

  Align F^* with V_G using peaks and cross zero points

  Resampling F^* to match with V_G

  $[CZ_{F^*}[1:n']] \leftarrow$ Find cross zero indexes F^*

  Segment $< F^*, V_G >$ pairs using cross zero indexes

  Obtain $N_c(areaID)$ /* trained network for all pairs using Bayesian back-propagation neural network */

  Navigate the antennas to the next area

return N_c

The movement-to-volume training is needed only once for each subject. During this process, a subject is asked to lie down and breath normally into a spirometer. The breathing volume V_G of the person is recorded. The patient's chest is spatially divided into subareas. Depending on the chest size and the beam width of the transmitting antenna, the number of areas, $gridSize$, is determined so that the antenna can beam to each area individually without overlapping to the others. Illustrated in Fig. 4, a chest is divided into 9 areas each of which is scanned sequentially by the antennas. For each area, F_I and F_Q signals are collected, along with the corresponding V_G. The training process is formalized in Alg. 2.

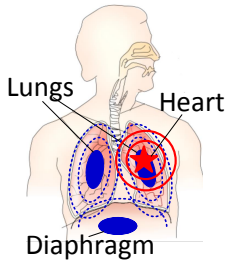

Fig. 6. Vibration sources including lung, heart, and diaphragm forced movement.

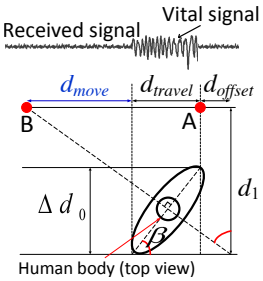

Fig. 7. Scanning process to identify the angle between the human body and the bed, β.

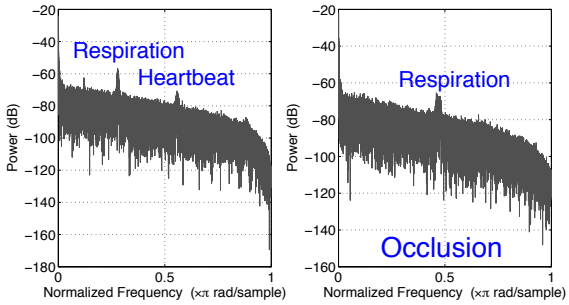

Fig. 8. An example illustrated the received signal when radar beams to human heart location without and with occlusion scenario.

Due to space limit, we refer readers to our technical report for further details and derivation of the training algorithm in [29].

D. Achievable Accuracy of Volume Estimator

We have implemented the basic volume estimating system (details in Sec. VI). Now we set up a simple scenario to verify the achievable accuracy of the technique and to identify possible optimization. The subject under test lies down on a bed and breaths normally for a period of 3 minutes, while his breathing volume are being monitored and estimated by both our WiSpiro and a spirometer (ground truth). At the beginning of the experiment, the person performs a 9-minutes-long training, following the procedure in Sec. IV-C.

Figure 5 plots the estimated volume time series. WiSpiro demonstrates a small mean error of $0.021l$, maximum error $0.052l$, and standard deviation $0.011l$ across the testing period.

V. Radar Navigator

The above analysis and experiment have shown that the basic WiSpiro is capable of estimating fine-grain breathing volume of a static subject. In this section, we describe a set of algorithms to make WiSpiro robust to disturbance caused by body movement in practical scenarios.

A. Posture Estimation

WiSpiro's posture estimation algorithm *estimates the current posture* of the user and changes the *location* and *beam direction* of the radar to ensure the chest movements are always captured by the radar receiver.

The respiration and heartbeat information are detectable when the radar beams to user's front chest. Meanwhile, those vital signs are difficult to capture when the radar beams to user's back. Exploiting those facts, we develop a scanning algorithm which mechanically brings the radar across the bed surface to scan and search for a position that senses vital signs. During the scanning, the radar transceivers are continuously running and pointing orthogonally to the bed. The collected signal is extracted to find the location where vital signs start and stop. Figure 7 plots the signals of an example scanning process, where the vital signs signature is detected. The radar is then navigated back to the middle point of the segment where vital signs were recognized, at $\frac{d_{travel}}{2}$ in Fig. 7. This simple step guarantees that the radar points to the frontal chest of the patient.

Next, WiSpiro navigates the radar to search for and beam to the heart location. Heart location is selected because the corresponding signal fluctuation contains both respiration and heartbeat information. However, it is nontrivial to automatically direct the radar from current location to the heart location. The required moving distance differs for different postures. For example, moving the radar from location 5 to 3 (Fig. 4) requires the radar to move its beam by 5 cm when the user is lying flat on bed (orthogonal to radar beam), but it requires only 4 cm when user body forms a 40 degree angle with the bed. In response, WiSpiro estimates the angle between the user's back and the bed to calculate the effective movement its beam would make on the chest surface given a fixed amount of movement on the radar. WiSpiro then directs the radar to different areas while capturing the signal at each moving step and stops at the location. Last, it identifies the heard area by finding the location that has the received signal that best matched with that of the heart location (Sec. V-B).

Estimating the angle between user's back and the bed surface. The key idea of estimating the angle is based on the gradient changes of vital signal strength on received signal. However, due to space limit, we refer readers to our technical report for further details and derivation of the algorithm in [29].

B. Point Localization

This section describes how WiSpiro recognizes the exact chest location the radar is beaming at. As can be seen in Figure 6 (a), human chest movement comprises 3 main sources: lungs, diaphragm, and heartbeat. Different areas move differently according to the distance to vibration sources, and the structure of muscles. We divide the chest into nine areas as in Figure 6 (b), named as $P1, P2, ..., P9$, respectively. This division depends on the radar beamwidth, its distance to chest, and the chest size. With a narrower beamwidth, the number of areas can be increased. On the other hand, the number of areas will be decreased if the system monitors young subjects with small chest (*e.g.* a baby). The key idea is to make sure the beam width is small enough to isolate the signal reflected from different areas. Moreover, as only a discrete set of areas

have been trained, we design an *interpolation* technique to fill up the data for untrained areas.

We use a machine learning technique to realize area recognition. Specifically, the radar beams a signal continuously, observes the signal features, and then match with those trained offline to identify the current area.

Due to space limit, we refer readers to our technical report for further details of the training process in [29].

VI. Testbed and System Implementation

In this section, we describe the WiSprio hardware and software that we implemented for evaluation purposes.

Hardware. As illustrated in Fig 9, the hardware setup is composed of two main components: a radio transceiver and a radar navigator. The *radio transceiver hardware* is developed from a iMotion radar [18], originally used for estimating respiratory rate. An iMotion transmitter sends single tone continuous wave at 2.4 GHz. A receiver captures reflected AC-coupled signals, convert to base band, and output discrete I/Q samples with 1 kHz baseband sampling rate. The received I/Q signals are transferred to a PC through a NI-DAQ 6008 module, to which our algorithms in Sec. IV and V are applied. One issue with the iMotion setup is that its antenna beamwidth of 60 degree is too wide to be usable for WiSpiro. We customize the antenna beamwidth by mounting tin cans on the patch surface, resulting in a narrower beaming angle of around 20 degrees.

The radio hardware is mounted on a mechanical motion control system from Cinetics [17] which is steered by a PC host in real-time. The control system supports 360° pan, tilt, and 64-inches slide movement. To navigate the radar to proper location and orientation, the motion control system is driven by our radar navigator algorithms (Sec. V) which are implemented on the PC host. The whole system is mounted across and on top of a twin-size bed on which all experiments are conducted.

Spirometer, camera, and microphone are used together to create ground-truth for various experimental verifications, to be detailed in Sec. VII.

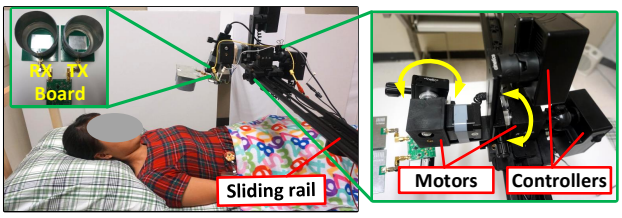

Fig. 9. WiSpiro setup.

Software.: We implement a program in Matlab to perform the training algorithms and volume estimation algorithm described in Sec. V. The radar controller software is developed and run in Matlab to realize posture estimation, point localization and associated training algorithms (Sec. V), and also make decisions on moving and steering antennas to proper location. We also developed a software using C++ to simultaneously trigger multiple hardware pieces at once to minimize the execution effort of the system and minimize the starting time discrepancy across the devices.

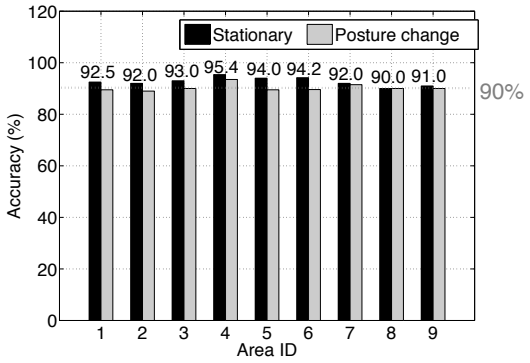

Fig. 10. The mean accuracy of volume estimation in two cases: users sleep stationary on the back, and users move during sleep.

VII. Performance Evaluation

A. Experiment Setup

Participants: To evaluate the performance of WiSpiro, we recruited 6 students (5 grads, 1 middle-school), with different weight, height, and a mean age of 25. During the experiments, a subject sleeps on the WiSpiro testbed (described in Sec. VI) wearing their normal clothes and covered by a thin blanket in some cases.

Ground truth: We use a spirometer [30] as a ground-truth to evaluate WiSpiro's volume estimation accuracy and train its algorithms when necessary. A camera was used to record participants' sleep behaviors and noise, together with a laser pointer to track the antenna's direction.

Training: The training process was done within 9 minutes for each participant. They were asked to breath normally to a spirometer when the radar was navigating and collecting data at all desired training areas.

Testing: After training, each participant was asked to sleep normally for about 60 mintues while WiSpiro is running. The spirometer was attached to the participant's mouth to collect ground-truth data.

B. Experiment Results and Analysis

Overall accuracy of breathing volume estimation. We group the testing results based on the ID of the area that the radar points to. Fig. 10 shows that, WiSpiro can estimate breathing volume with 90% to 95.4% accuracy, which mean the error is less than 10% of the total breathing volume within an average window of 10ms. The performance peaks at areas on upper part of the chest and around the heart area. The results also show that the impact of body and limb motion is small, thanks to the radar navigator algorithms.

Potential medical significance of WiSpiro. We evaluate the medical implication and benefit from WiSpiro, focusing on a specific question: *Could WiSpiro provide meaningful information to help clinical doctor in sleep and respiratory disease diagnosis?*

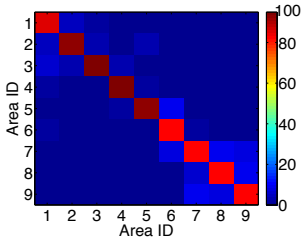

Fig. 11. The accuracy distribution of point localization technique

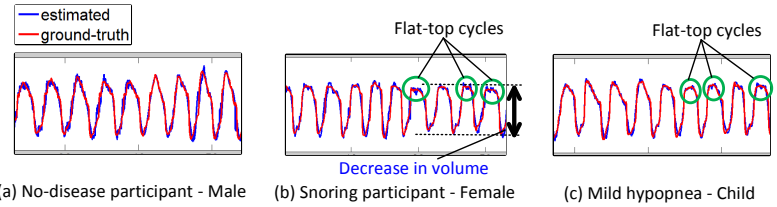

Fig. 12. The example volume signal of the three participants with and without breathing and sleep diseases. Flat-top breathing cycles and the decrease in volume are features that are identified and used by clincal doctor for diagnosis.

We recruited 3 volunteers: one male middle-school intern student with known minor hypopnea, one normal male student, one female student with a known mild snoring pattern. The three subjects' breathing volume, which is monitored by both a spirometer and WiSpiro, are given to a clinical doctor, a sleep expert who directs and operates a clinical sleep analysis lab in a state hospital.

From the fine-grained breathing information, the doctor was able to map the breathing volume pattern to each person without prior knowledge about the mapping. Once the symptom is confirmed, the doctor was able to provide further analysis of breathing and sleeping issues from the volume information, part of which is presented in Fig. 12 (b). *"With a known snoring female, the signal shows a small inspiratory flow limitation but very little effect on her tidal volume. This is a marker of mild flow limitation that is commonly seen in premenopausal woman. It is likely a non-REM sleep because of the regular rate. The normal volume variability which can normally be seen through CO_2 and O_2 levels.",* said the doctor regarding the female subject with mild-snoring. The flat top of part of the volume measurement, marked in Fig. 12, is an indication of flow limitation which is, otherwise, not possible to be captured with breathing rate information.

Regarding to the middle school student's breathing volume time series, the doctor analyzed as follows: *"These three breathing cycles (the doctor was pointing to the part marked on Fig. 12 (c)) show a moderate inspiratory flow limitation that decreases the tidal volume of the breath. This could be clinically important because the child might get enough O_2 due to the air flow limitation and decreased volume. This could lead to alteration of blood gas such as CO_2 and O_2 levels. The moderate flow limitation during sleep is one form of hypopnea"*. Once again, this analysis mostly relies on the breathing volume and its variation overtime, which is not acquirable from respiration rate.

While this qualitative analysis is not statistically significant to make a conclusive answer for the aforementioned question, it shows that WiSpiro's accurate and fine-grained breathing volume information is potentially useful for medical practice.

Accuracy of point localization technique. We now evaluate the accuracy of WiSpiro's point localization module and its impacts on the system's overall performance. After training, we beam the antennas to different areas on each participant. We repeat the process for 15 times at each area for all 9 participants. The accuracy is then averaged across participants. Fig. 14 shows the accuracy of the algorithm in

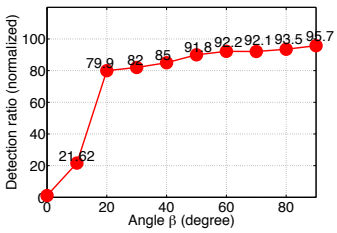

Fig. 13. Estimation accuracy of the angle between human back and the bed surface

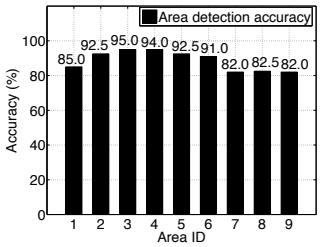

Fig. 14. Chest area ID detection accuracy

correctly detecting the area ID. The results show that the algorithm performs better in detecting areas that are close to the heart, position 2, 3, 4, and 5, while accuracy drops near the abdominal area. This trend is intuitive since there are more vital signal affects on the former set of areas. Fig. 11 shows the error distribution of the localization. It shows that when an error happens, it tends to be confused with an area with its neighborhood.

Accuracy of posture detection. The performance of our posture detection algorithm is presented in Fig. 13. A participant is asked to lie his/her body w.r.t. the bed with an angle ranging from 10^o to 90^o with step of 10^o. The estimation is repeated 20 times for each participant at each angle. The results show that WiSpiro can roughly estimate the angle of more than 20 degree with the accuracy of 80% versus only 21.62% accuracy when the angle is at 10 degree. The angle is considered to be correctly estimated if the result is within 5% from the ground truth. This limitation is due to the wide beam angle of our antenna at 20^o. As the angle increases, the posture detection accuracy increases up to 95.7%.

VIII. Related Works

Radar technique has been widely used in estimating vital signs. The frequency and phase shift of body-reflected radar signals have be used to estimated the heart and breathing rate [19], [21], [22], [24]. Droidcour *et al.* [10] introduce a linear correlation model to approximate the chest movement based on phase information. Linearity holds only if the movement is much smaller compared with the wavelength so that the chest movement is linearly proportional to the phase change. Using this approach, breathing rate and heart beat can be extracted by analyzing the received signal on frequency domain. Changi *et al.* [11] analyze the breathing activities using Fourier series and exploit the harmonics information to obtain the respiration rate and heart beat regardless of the distance from subject to radar. The dependency of movement and wavelength of

the signal has also been resolved. Adib [13] used FMCW technique to collect the change of distance between radar to multiple objects and infer their breathing rates based on the traveling time of the signal. These approaches triggered substantial investigation along the same line. In addition, Patwari *et al.* [22] presented the feasibility of using Wi-Fi of the shelf device to track respiration rate in real time. However, breathing rate estimation, a problem equally important to medical practitioners, has not been thoroughly solved. Early efforts in tidal volume estimation (*e.g.*, [26]) focused on controlled settings and short-term monitoring, which is of less clinical significance as discussed in Sec. I. To our knowledge, WiSpiro marks the first step to systematically investigate the problem under practical settings involving body area heterogeneity, random body movement, etc.

IX. Limitations and Future Work

WiSpiro relies on the correlation between breathing volume and chest movement of a human body. The system might not perform well in scenarios where that assumption does not hold. While it rarely happens, there exist a few of such cases. One example is apnea caused by blockage in the respiratory airway of the patient. Regardless of the apnea patient's effort in inhaling or exhaling, the breathing volume does not change since no air can go through the airway, while the chest and other frontal areas might still be moved by the pressure caused by the respiratory effort. One possible solution to detect this is to combine WiSpiro with a sensing system that could capture inhaling and exhaling air flow, such as CO_2, O_2 levels, or thermal camera.

WiSpiro's scanning process is currently taking tens of seconds due to limitations of the mechanical motion control system. The scanning will suffer further if the subject moves frequently during scanning, in which case, the scanning process need to be reset. This limitation can be overcome by using a more efficient motion control system, combined with electronically steerable phased-array antennas. Finally, our experimental results are performed on a small user population. More thorough testing with in-house and in-hospital setup could further validate the clinical significance of WiSpiro. We consider that as extension of this work.

X. Conclusion

We have presented WiSpiro, the first autonomous radar system to monitor breathing volume of a sleeping person. WiSpiro achieves fine-grained volume estimation using a phase-motion model, combined with a neural network training that maps chest movement to breathing volume, taking into account heterogeneity of frontal body areas. Further, WiSpiro handles random body movement, by redirecting the radar in real-time, using a set of navigation and area localization algorithms. Our prototype and experiments verify WiSpiro's feasibility, and its ability to track breathing volume at high accuracy. Our immediate next step of research is to optimize WiSpiro and test it in practical clinical environment.

References

[1] R. Balkissoon et al., *Chronic obstructive pulmonary disease: a concise review*. The Medical Clinics of North America, 2011.

[2] Kurl S, Jae SY, Kauhanen J, Ronkainen K, Laukkanen JA. *Impaired pulmonary function is a risk predictor for sudden cardiac death in men*. Ann Med. 2015.

[3] Pregnancy and sleep. http://sleepfoundation.org/sleep-topics/pregnancy-and-sleep.

[4] Facco FL et. al., *Sleep disordered breathing in a high-risk cohort prevalence and severity across pregnancy*. Am J Perinatol. 2014. doi: 10.1055/s-0033-1363768.

[5] Marcus CL, et. al., *American Academy of Pediatrics. Diagnosis and management of childhood obstructive sleep apnea syndrome*. Pediatrics. 2012 Sep;130(3):576-84. doi: 10.1542/peds.2012-1671.

[6] Mannarino MR et. al., *Obstructive sleep apnea syndrome*. Eur J Intern Med. 201. doi: 10.1016/j.ejim.2012.05.013.

[7] Halbower AC et. al., *Childhood obstructive sleep-disordered breathing: a clinical update and discussion of technological innovations and challenges*. Chest. 2007.

[8] L. Boccanfuso and J. OKane. *Remote measurement of breathing rate in real time using a high precision, single-point infrared temperature sensor*. IEEE BioRob, 2012.

[9] Y. Ren et. al., *Fine-grained Sleep Monitoring: Hearing Your Breathing with Smartphones*, IEEE INFOCOM, 2015.

[10] A. Droitcour et al., *Range correlation and I/Q performance benefits in single-chip silicon doppler radars for noncontact cardiopulmonary monitoring*. IEEE Trans. on Micro. Theory Techn., 2004.

[11] L. Lu et al., *Doppler radar noncontact vital sign monitoring.* Neural Comp., Neural Devices, and Neural Prosthesis, 2014.

[12] R. Nandakumar et. al., *Contactless sleep apnea detection on smartphones.* ACM Mobisys, 2015

[13] F. Adib et. al., *Smart homes that monitor breathing and heart rate.* ACM CHI, 2015.

[14] J. Liu et. al, *Tracking Vital Signs During Sleep Leveraging Off-the-shelf WiFi*, ACM MobiHoc, 2015.

[15] Mackay DJC. *Bayesian methods for adaptive models.* PhD Thesis, California Institute of Technology, 1991.

[16] Neal RM. *Bayesian training of back-propagation networks by the hybrid Monte Carlo method*. Technical Report CRG-TG-92-1, Department of Computer Science, University of Toronto, 1992.

[17] Cinetics. http://cinetics.com/axis360/

[18] Yiran Li et. al., *Wireless Radar Devices for Smart Human-Computer Interaction*, IEEE MWSCAS, pp 65–68, 2014.

[19] W. Massagram et. al., *Microwave Non-invasive Sensing of Respiratory Tidal Volume*, Annu. IEEE Int.Eng. Med. Biol. Soc. Conf., pp 4832-4835, 2009.

[20] T. Kondo et. al., *Laser monitoring of chest wall displacement*, European Respiratory Journal, pp 1865-1869, 1997.

[21] F. Adib et. al., *3D tracking via body radio reflection*, Proceedings of the 11th USENIX Conference on Networked Systems Design and Implementation, pp 317-329, 2014.

[22] N. Patwari et. al., *Breathfinding: A wireless network that monitors and locates breathing in a home*, IEEE Journal of Selected Topics in Signal Processing, pp 30-42, 2014.

[23] A. D. Groote et. al., *Chest wall motion during tidal breathing*, Journal of Applied Physiology, pp 1531-1537, 1997.

[24] Y-J. An et. al., *Detection of Human Vital Signs and Estimation of Direction of Arrival Using Multiple Doppler Radars*, Journal of the Korean Institute of Electromagnetic Engineering and Science, Vol. 10, No. 4, pp 250-255, 2010.

[25] M.-C. Yu et. al., *Noncontact Respiratory Measurement of Volume Change Using Depth Camera*, 34th Annu. IEEE Int.Eng. Med. Biol. Soc. Conf., pp. 2371-2374, 2012.

[26] W. Massagram et. al., *Tidal Volume Measurement Through Noncontact Doppler Radar with DC Reconstruction*, IEEE Sensors Journal, Vol. 13, No. 9, pp. 3397-3404, 2013.

[27] A. H. Madsen et. al., *Signal Processing Methods for Doppler Radar Heart Rate Monitoring*, Signal Processing Techniques for Knowledge Extraction and Information Fusion, pp. 121-140, 2008.

[28] J. Vargas and C. O. S. Sorzano, *Quadrature Component Analysis for interferometry*, Optics and Lasers in Eng., pp. 637-641, 2013.

[29] Technical Report. http://tinyurl.com/hmldpg3

[30] Spirometer. http://www.vernier.com/products/sensors/spr-bta/